Hindawi Publishing Corporation
EURASIP Journal on Wireless Communications and Networking
Volume 2011, Article ID 761369, 9 pages
doi:10.1155/2011/761369

Research Article

Error Probability of DPPM UWB Systems over Nakagami Fading Channels with Receive Diversity

Hao Zhang,[1,2] Ting-ting Lu,[1] Jing-jing Wang,[1] and T. Aaron Gulliver[2]

[1] *Department of Electrical Engineering, Ocean University of China, Qingdao 266100, China*
[2] *Department of Electrical and Computer Engineering, University of Victoria, Victoria, BC, Canada V8W 3P6*

Correspondence should be addressed to Hao Zhang, zhanghao@ouc.edu.cn

Received 5 May 2010; Accepted 13 February 2011

Academic Editor: T. D. Abhayapala

We consider differential-pulse position modulation (DPPM) in an ultra wideband (UWB) communication system. A typical format for a DPPM signal in a UWB system is derived from that of a pulse position modulation (PPM) signal. The error probabilities of a UWB DPPM system with receive diversity over additive white Gaussian noise (AWGN) and Nakagami fading channels are derived. Both single-user and multiuser environments are considered. Performance results are presented which show that the frame error rate (FER) with DPPM is better than that with PPM, and the FER performance can be improved significantly by receive diversity.

1. Introduction

PPM has been used extensively in optical communication systems and is the modulation employed in the IEEE 802.11 infrared physical layer standard [1]. However, PPM adds complexity to the system since both slot and symbol synchronization are required at the receiver in order to demodulate the incoming signal [2]. Thus DPPM has been proposed as an alternative to PPM [3, 4]. DPPM provides a higher transmission capacity by deleting redundant slots in a symbol. It does not require symbol synchronization since each symbol ends with a "1" pulse.

In recent years, DPPM has drawn wide attention as a promising modulation scheme for optical and short range radio communication. In [5], the code properties and spectral characteristics of a type of DPPM called digital pulse interval modulation (DPIM) were discussed. The probability of error with DPIM in optical wireless communication systems was also presented; in [6], the packet error rate (PER) was derived for a simple threshold detection-based receiver. It was shown that the PER of DPPM for a given average received irradiance was superior to that with on-off keying (OOK), but PPM was better than DPPM. For a given bandwidth, DPPM was shown in [7] to require significantly less average power than PPM. The performance of DPPM in the presence of multipath intersymbol interference (ISI) was also examined. A hybrid modulation technique called differential amplitude pulse position modulation (DAPPM) was recently proposed in [8]. DAPPM is a combination of pulse amplitude modulation (PAM) and DPPM. The symbol structure and properties of DAPPM, for example, peak-to-average power ratio (PAPR), bandwidth requirements, and throughput, were compared with other techniques such as DPIM.

Most research on DPPM considers only optical communication systems. This paper examines DPPM for use in UWB systems. The typical format of a DPPM signal in a UWB system is derived, and the error probabilities over AWGN and Nakagami fading channels are derived. Both single-user and multiuser environments are considered. Receive diversity is employed in the UWB system to improve performance. This can be achieved using a RAKE receiver or multiple receive antennas.

The remainder of this paper is organized as follows. In Section 2, the signal construction and system model over Nakagami fading channels are introduced. Section 3 presents the error probability analysis of the DPPM UWB system over both AWGN and Nakagami fading channels in a single-user

environment. The performance of the DPPM system in a multiuser environment is analyzed in Section 4. Numerical results on the system performance are given in Section 5. Finally, some conclusions are given in Section 6.

2. Signal Construction and System Model over Nakagami Fading Channels

2.1. Signal Construction and System Model. DPPM is a simple modification of PPM that can provide improved power and/or bandwidth efficiency [7]. In this paper, we consider a multiuser UWB system. The M-ary PPM signal set for the kth user is $\{s_1^{(k)}(t), s_2^{(k)}(t), \ldots, s_m^{(k)}(t)\}$, where $s_m^{(k)}(t)$ $(1 \le m \le M)$ can be written as [9]

$$s_m^{(k)}(t) = \sum_{j=0}^{N_s} \sqrt{E_p}\, p\left(t - jT_f - c_j^{(k)} T_c - \delta_{d^{(k)}_{\lfloor j/N_s \rfloor}}\right), \tag{1}$$

where N_s is the number of pulses that form a data symbol, $p(t)$ is the UWB pulse of duration T_p, and E_p is the energy per pulse. The pulse repetition interval is T_f. c_j is the time-hopping code, and δ is the PPM time shift, where we assume $\delta_1 = 0, \delta_1 < \delta_2 < \cdots < \delta_M < T_f$.

Without loss of generality, we assume unit signal amplitude, that is, $\sqrt{E_p} = 1$ and if the time-hopping code is ignored $(c_j = 0)$, the M-ary PPM signal can be expressed as

$$s^{(k)}(t) = \sum_{j=-\infty}^{\infty} p\left(t - jT_f - a_j^{(k)} T\right), \tag{2}$$

where $a_j \in \{0, 1, \ldots, M-1\}$ and T is the time slot duration.

A DPPM symbol is obtained from the corresponding PPM symbol by deleting all of the "0" slots that follow the "1" slot, as shown in Table 1. In contrast to PPM, where a symbol has fixed length M, the DPPM format generates a variable-length symbol since the "0"s after the "1" have been dropped.

The jth DPPM symbol is B_j with symbol length determined by the data being encoded, that is, $\lambda_j = a_j + 1$. The cumulative length Λ_j in DPPM is defined as

$$\Lambda_j = \begin{cases} \sum_{k=0}^{j-1} \lambda_k & j > 0, \\ 0 & j = 0, \end{cases} \tag{3}$$

so that $\Lambda_j T$ represents the beginning of the jth symbol. Thus, the M-ary DPPM signal can be written as

$$s^{(k)}(t) = \sum_{j=-\infty}^{\infty} p\left(t - \Lambda_j T - a_j^{(k)} T\right). \tag{4}$$

Table 1: Comparison of Symbol Mapping for 4PPM and 4DPPM.

a_j	4PPM		4DPPM	
	Symbol B	Length λ	Symbol B	Length $\lambda = a + 1$
0	1000	4	1	1
1	0100	4	01	2
2	0010	4	001	3
3	0001	4	0001	4

The received signal can be modeled as the derivative of the transmitted pulses assuming propagation in free space [10]

$$\begin{aligned} r(t) &= \sum_{l_d=1}^{L_d} \sum_{k=1}^{N_u} \left[\left(s^{(k)}(t - \tau_{l_d k}) \right)' + w_{l_d}(t) \right] \\ &= \sum_{l_d=1}^{L_d} \left[\sum_{k=1}^{N_u} \sum_{j=-\infty}^{\infty} q\left(t - \Lambda_j T - a_j^{(k)} T - \tau_{l_d k}\right) + w_{l_d}(t) \right], \end{aligned} \tag{5}$$

where $w_{l_d}(t)$ is AWGN with power spectral density $N_0/2$, $\tau_{l_d k}$ is the propagation delay of the signal sent by the kth user, $q(t)$ is the received pulse waveform, and L_d is the receive diversity order. Receive diversity can be achieved using a RAKE receiver or multiple receive antennas. For simplicity, we employ equal gain combining (EGC) at the receiver in the following discussion.

2.2. The Statistical Model for Nakagami Fading Channels. The propagation model for Nakagami fading channels can be described by the channel impulse response [11]

$$h(t) = \sum_{l=1}^{L} f_l(t)\delta(t - \tau_l(t)), \tag{6}$$

where t is the observation time, L is the number of resolvable paths, $\tau_l(t)$ is the arrival-time of the received signal via the lth path which is log-normal distributed [9], $f_l(t)$ is the random time-varying amplitude attenuation, and δ denotes the Dirac delta function. Without loss of generality, $\tau_l(t)$ is defined such that $\tau_1 < \tau_2 < \cdots < \tau_L$. The attenuation, $f_l(t)$, can be expressed as $f_l(t) = v_l f_l$ with $v_l = \text{sign}(f_l)$ and $f_l = |f_l(t)|$ which is the magnitude of $f_l(t)$. The PDF of this magnitude is given by [11]

$$p(f_l) = \frac{2}{\Gamma(m)} \left(\frac{m}{\Omega_l}\right)^m f_l^{2m-1} e^{-m f_l^2/\Omega_l} m, \tag{7}$$

where $\Gamma(\cdot)$ denotes the Gamma function, $\Omega_l = E[f_l^2]$, and $m = E[f_l^2]/\text{var}[f_l^2]$ with $m \ge 1/2$. To make the channel characteristics analyzable without affecting the generality of the channel, we further define v_l as a random variable that takes the values +1 or −1 with equal probability.

3. Error Probability Analysis of a Single-User DPPM System

3.1. Error Probability of M-ary DPPM over AWGN Channels. EGC is assumed at the receiver, so the received signal can be expressed as

$$\mathbf{r} = \sum_{l_d=1}^{L_d} (\mathbf{s} + \mathbf{w}_{l_d}) = L_d \mathbf{s} + \sum_{l_d=1}^{L_d} \mathbf{w}_{l_d}. \tag{8}$$

To evaluate the error probability of M-ary DPPM, we suppose that signal s_N is transmitted. The vector representation for an M-ary DPPM signal is defined as an N-dimensional vector with nonzero value in the Nth dimension $s_N = [0, \ldots, 0, \sqrt{E_s}]$. Then the received signal vector over an AWGN channel is

$$\mathbf{r} = \left[\sum_{l_d=1}^{L_d} n_{l_d 1} \sum_{l_d=1}^{L_d} n_{l_d 2} \cdots L_d \sqrt{E_s} + \sum_{l_d=1}^{L_d} n_{l_d N} \right], \tag{9}$$

where E_s is the energy in a symbol, and $n_{l_d 1} n_{l_d 2}, \ldots, n_{l_d N}$ are zero-mean, mutually statistically independent Gaussian random variables with equal variance $N_0/2$. In this case, the outputs from the bank of M correlators are

$$\begin{aligned} C(\mathbf{r}, \mathbf{h}_1) &= \sqrt{E_s} n_1, \\ C(\mathbf{r}, \mathbf{h}_2) &= \sqrt{E_s} n_2, \\ &\vdots \quad \vdots \\ C(\mathbf{r}, \mathbf{h}_N) &= \sqrt{E_s} \left(L_d \sqrt{E_s} + n_N \right), \\ C(\mathbf{r}, \mathbf{h}_{N+1}) &= 0, \\ &\vdots \quad \vdots \\ C(\mathbf{r}, \mathbf{h}_M) &= 0, \end{aligned} \tag{10}$$

where $n_N = \sum_{l_d=1}^{L_d} n_{l_d N}$. Thus $n_1, n_2, \ldots, n_N$ are zero-mean, mutually statistically independent Gaussian random variables with equal variance $L_d N_0/2$.

The PDF of the Nth correlator output is

$$p(r_N) = \frac{1}{\sqrt{\pi L_d N_0}} \exp\left(-\frac{(r_N - L_d \sqrt{E_s})^2}{L_d N_0} \right), \tag{11}$$

and the PDFs of the other $N-1$ correlator outputs are

$$p(r_m) = \frac{1}{\sqrt{\pi L_d N_0}} \exp\left(-\frac{r_m^2}{L_d N_0} \right), \quad m = 1, 2, \ldots, N-1. \tag{12}$$

The probability that the detector makes a correct decision is then

$$P_c = \int_{-\infty}^{\infty} P(n_1 < r_N, n_2 < r_N, \ldots, n_{N-1} < r_N \mid r_N) p(r_N) dr_N. \tag{13}$$

Since $\{r_m\}$ are statistically independent, the joint probability factors into a product of $N-1$ marginal probabilities of the form

$$\begin{aligned} &p(n_m < r_N \mid r_N) \\ &\quad = \int_{-\infty}^{\infty} p_{r_m}(x_m) dx_m = \frac{1}{\sqrt{2\pi}} \\ &\qquad \times \int_{-\infty}^{r_N \sqrt{2/(L_d N_0)}} e^{-x^2/2} dx \quad m = 1, 2, \ldots, N-1, \end{aligned} \tag{14}$$

so that

$$P_c = \int_{-\infty}^{\infty} \left(\frac{1}{\sqrt{2\pi}} \int_{-\infty}^{r_N \sqrt{2/L_d N_0}} e^{-x^2/2} dx \right)^{N-1} p(r_N) dr_N. \tag{15}$$

The probability of a symbol error is

$$P_M = 1 - P_c, \tag{16}$$

therefore

$$\begin{aligned} P_M = \frac{1}{\sqrt{2\pi}} \int_{-\infty}^{+\infty} &\left[1 - \left(\frac{1}{\sqrt{2\pi}} \int_{-\infty}^{y} e^{-x^2/2} dx \right)^{N-1} \right] \\ &\times \exp\left[-\frac{1}{2} \left[y - \sqrt{\frac{2L_d E_s}{N_0}} \right]^2 \right] dy. \end{aligned} \tag{17}$$

With M-ary PPM, assuming the M possible signals are equally likely and orthogonal, it is possible to convert the probability of symbol error into a corresponding probability of bit error using [12]

$$P\,(\text{bit error}) = \frac{2^{k-1}}{2^k - 1} P\,(\text{symbol error}). \tag{18}$$

In DPPM, the pulses define the symbol boundaries, so an error is not confined to the symbol in which the error occurs. Consider a frame of data encoded using DPPM. A pulse detected in the wrong slot will affect both symbols either side of the pulse, but have no influence on the remaining symbols in the frame. A pulse not detected or detecting an additional pulse results in a shift of the remaining symbols in the frame. Thus, the conversion given in (18) is inaccurate for DPPM. In order to compare the performance of DPPM with that of PPM, we base our analysis on the FER. A frame is considered to be in error if one or more of symbols within the frame are in error. This can be expressed as [13]

$$P_{\text{FE}} = 1 - \prod_{n=1}^{Y} (1 - P_{\text{SE}_n}), \tag{19}$$

where P_{FE} is the probability of frame error, Y is the number of symbols in a frame, and P_{SE_n} is the probability that the nth symbol is in error.

3.2. Error Probability of M-ary DPPM over Nakagami Fading Channels

3.2.1. Equivalent Instantaneous SNR. With a single-user active in the system, the received signal with attenuation due to Nakagami fading and with receive diversity can be written as

$$r(t) = \sum_{l_d=1}^{L_d} \left(f_{l_d}(t)\delta\left(t - \tau_{l_d}(t)\right)X(t) + w_{l_d}(t)\right), \tag{20}$$

where $X(t) = (s(t))' = \sum_{j=-\infty}^{\infty} q(t - \Lambda_j T - a_j T)$. The equivalent instantaneous SNR of (20) is given by [14]

$$\rho = \frac{\int_{-W/2}^{W/2} G_X(f)\,|H(f)|^2 df}{N_0 W}, \tag{21}$$

where $G_X(f)$ is the power spectral density (PSD) of the UWB signal determined by the pulse shape and modulation employed and $H(f)$ is the PSD of $h(t)$ given by

$$H(f) = \sum_{l_d=1}^{L_d} \nu_{l_d} f_{l_d} e^{-j2\pi f(l_d-1)\tau}. \tag{22}$$

Without loss of generality, we assume $X(t)$ has a uniformly distributed PSD, that is

$$G_X(f) = \begin{cases} \dfrac{P_x}{W}, & \text{where } f \in \left[-\dfrac{W}{2} \quad \dfrac{W}{2}\right], \\ 0, & \text{otherwise}, \end{cases} \tag{23}$$

where P_x is the power of the received UWB signal. Equation (21) can then be written as

$$\rho = \rho_s \frac{1}{\pi} \int_0^{\pi} \left[\left(\sum_{l_d=1}^{L_d} \nu_{l_d} f_{l_d} \cos((l_d - 1)u) \right)^2 + \left(\sum_{l_d=1}^{L_d} \nu_{l_d} f_{l_d} \sin((l_d - 1)u) \right)^2 \right] du, \tag{24}$$

where $\rho_s = P_x/(WN_0)$ is the symbol SNR of the UWB system over an AWGN channel. The equivalent SNR ρ is the symbol SNR modified according to the number of paths and the fading coefficients.

3.2.2. Error Probability over Nakagami Fading Channels. The error probability of M-ary DPPM over an AWGN channel (17) can be expressed as

$$P_M = \frac{1}{\sqrt{2\pi}} \int_{-\infty}^{+\infty} \left[1 - \left(\frac{1}{\sqrt{2\pi}} \int_{-\infty}^{y} e^{-x^2/2} dx \right)^{N-1} \right] \times \exp\left[-\frac{1}{2}\left[y - \sqrt{\rho_s} \right]^2 \right] dy. \tag{25}$$

With a simple variable transformation, the error probability of M-ary DPPM over Nakagami fading channels can be obtained by substituting ρ for ρ_s in (25). The probability of frame error can then be expressed as (19).

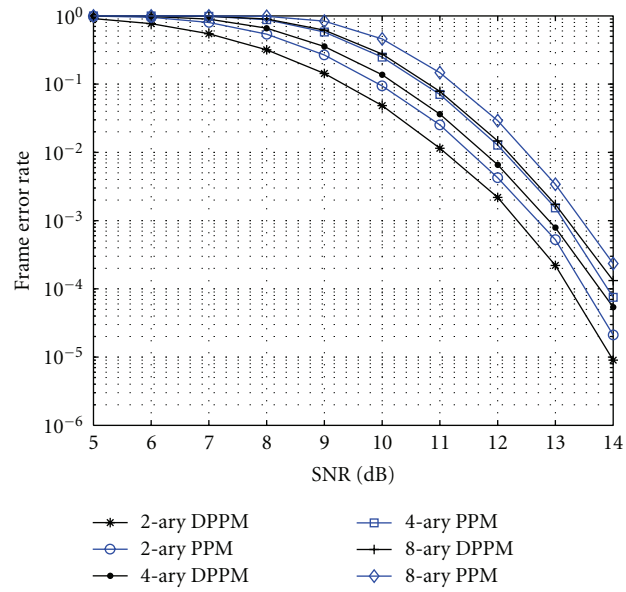

Figure 1: Frame error rate for PPM and DPPM over an AWGN channel with a frame length of 128 bits.

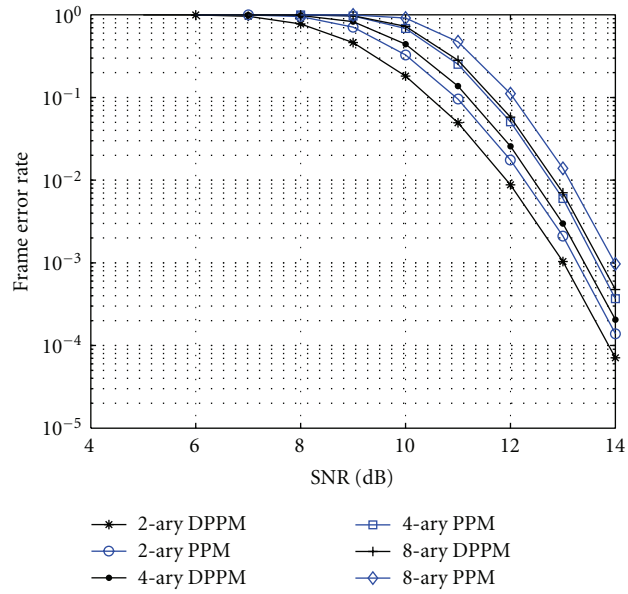

Figure 2: Frame error rate for PPM and DPPM over an AWGN channel with a frame length of 512 bits.

4. Error Probability Analysis of a Multiuser DPPM System

With more than one user active in the system, multiple access interference (MAI) is the major factor limiting performance. The net effect of the MAI produced by the undesired users at the output of the desired user's correlation receiver can be modeled as a zero-mean Gaussian random variable if the number of users is large or a repetition code is used with $N_s \gg 1$ [15]. Based on the multiple access error probability of M-ary PPM [14], in this section, the multiple access error

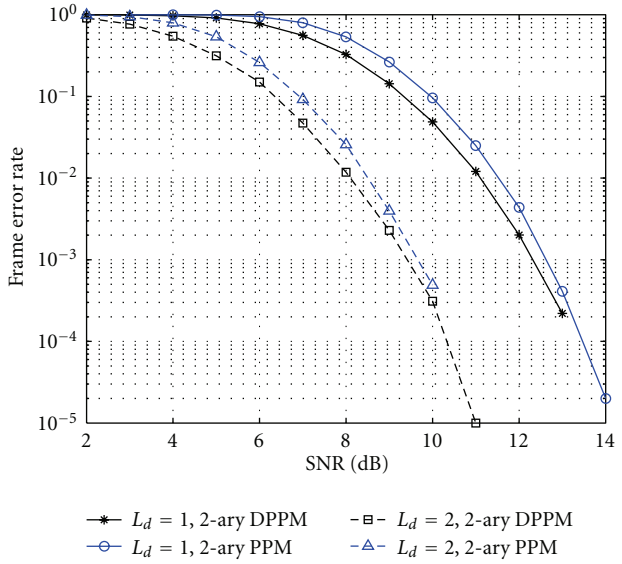

Figure 3: Frame error rate for binary PPM and binary DPPM with receive diversity order $L_d = 1, 2$, and a frame length of 128 bits over AWGN channels.

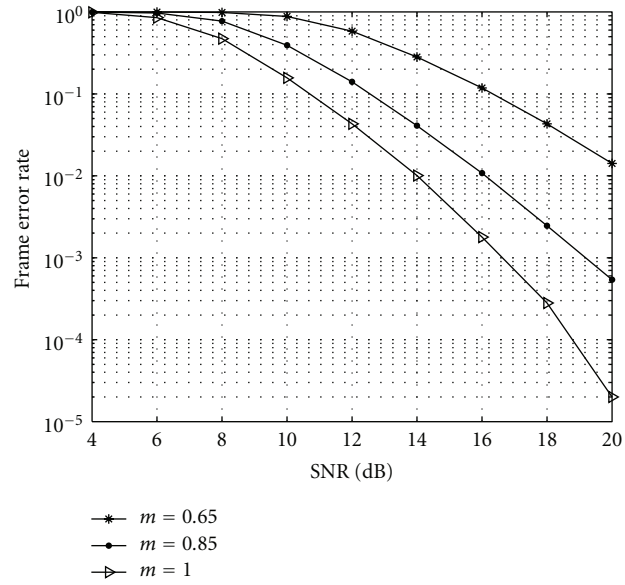

Figure 4: Frame error rate for 4-ary DPPM over Nakagami fading channels with different m, a frame length of 128 bits and receive diversity order $L_d = 4$.

probability of DPPM system is investigated. By modifying the noise distribution, the error probability analysis given in Section 3 for a single-user can be extended to multiple access systems.

4.1. Multiple Access Error Probability over AWGN Channels

4.1.1. Multiple Access Interference Model. The received signal is modeled as in (5) so that

$$r(t) = \sum_{l_d=1}^{L_d} \sum_{k=1}^{N_u} \left[\left(s_l^{(k)}(t - \tau_{l_d k}) \right)' + w_{l_d}(t) \right]. \tag{26}$$

Without loss generality, we assume the desired user corresponds to $k = 1$. The single-user optimal receiver is an M-ary pulse correlation receiver followed by a detector. We assume the receiver is perfectly synchronized to user 1 since each symbol ends with a "1" pulse, that is, $\tau_{l_d k}$ is known. The M-ary cross-correlation receiver for user 1 consists of M filters matched to the basis functions defined as

$$\varphi_{al_d}^{(1)} = q\left(t - a^{(1)}T - \tau_{l_d 1}\right) \quad a = 1, \ldots, M. \tag{27}$$

The output of each cross-correlation receiver for the sample period $[nN_sT_f \quad (n+1)N_sT_f]$ is

$$\mathbf{r}_i = \sum_{j=nN_s+1}^{(n+1)N_s} \int_{(j-1)T_f}^{jT_f} r(t)\varphi_{al_d}^{(1)}\left(t - \Lambda_j T\right)dt, \tag{28}$$

which can be written as

$$\mathbf{r}_i = \begin{cases} L_d N_s \sqrt{E_p^{(1)}} + W_I + W, & \text{signal}, \\ W_I + W, & \text{no signal}, \end{cases} \tag{29}$$

where W_I is the MAI component given by

$$W_I = \sum_{l_d=1}^{L_d} \sum_{k=2}^{N_u} \sum_{j=nN_s+1}^{(n+1)N_s} \int_{(j-1)T_f}^{jT_f} \sqrt{E_p^{(k)}} q\left(t - \Lambda_j T - a_j^{(k)} T - \tau_{l_d k}\right) \times q\left(t - \Lambda_j T - a_j^{(1)} T - \tau_{l_d 1}\right) dt \tag{30}$$

and W is the AWGN component

$$W = \sum_{l_d=1}^{L_d} \sum_{j=nN_s+1}^{(n+1)N_s} \int_{(j-1)T_f}^{jT_f} w_{l_d}(t) q\left(t - \Lambda_j T - a_j^{(1)} T - \tau_{l_d 1}\right) dt. \tag{31}$$

By defining the autocorrelation function of $q(t)$ as

$$\gamma(\Delta) = \int_0^{T_f} q(t)q(t - \Delta)dt, \tag{32}$$

equation (30) can be written as

$$W_I = \sum_{l_d=1}^{L_d} \sum_{j=1}^{N_s} \sum_{k=2}^{N_u} \sqrt{E_p^{(k)}} \gamma(\Delta), \tag{33}$$

where Δ is the time difference between user 1 and k, which can be expressed as

$$\Delta = \left(a_j^{(1)} - a_j^{(k)}\right) T + (\tau_{l_d 1} - \tau_{l_d k}). \tag{34}$$

Assuming that each user has a uniformly distributed data source, the probability of any M-ary PPM symbol is $1/M$, and the data sequences for the users are independent. Hence the $a_j^{(k)}$ are independent and identically distributed

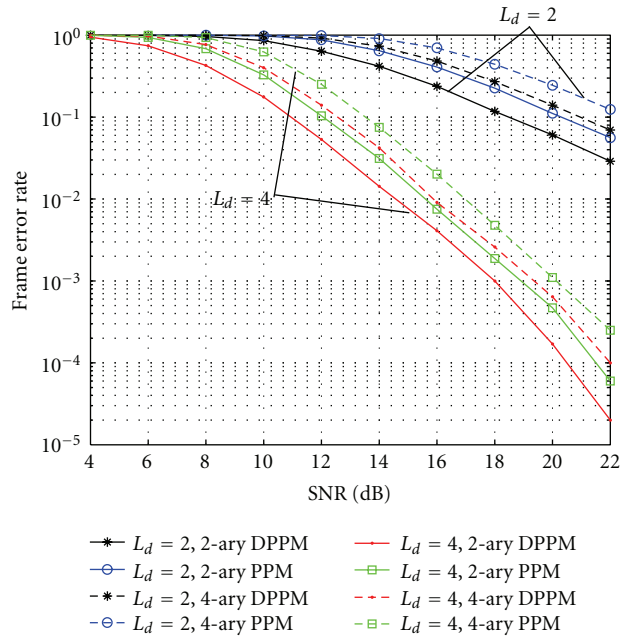

FIGURE 5: Frame error rate for M-ary PPM and M-ary DPPM with receive diversity order $L_d = 2, 4$ and a frame length of 128 bits over a Nakagami fading channel, $m = 0.85$.

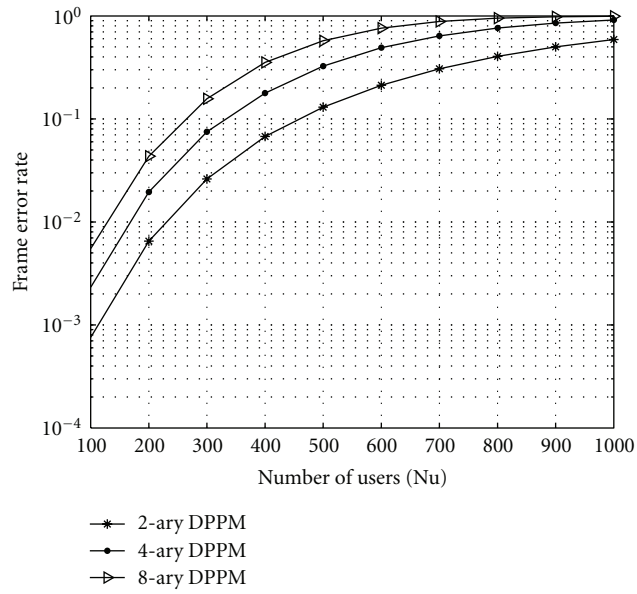

FIGURE 6: Relationship between frame error rate and number of users for M-ary DPPM with receive diversity $L_d = 4$, and a frame length of 128 bits over an AWGN channel, $\beta = 500$, SNR = 8 dB.

(i.i.d.) random variables. $\tau_{l_d k}$ is also assumed to be an i.i.d. uniformly distributed random variable over the symbol interval. Thus, Δ can be modeled as a random variable uniformly distributed over $[-T_f, T_f]$. The MAI in a multiple access UWB system with DPPM is similar to that with PPM. As in [10, 15, 16], the MAI is modeled as a Gaussian random process for the multiuser environment. The mean and variance of the MAI component are determined by the specific pulse waveform [16]. For simplicity, we consider a UWB system utilizing a rectangular waveform. The UWB pulse $q(t)$ is then defined as

$$q(t) = \sqrt{\frac{1}{T_p}} \quad 0 \le t \le T_p. \tag{35}$$

The autocorrelation function of $q(t)$ is

$$\gamma(\Delta) = \begin{cases} \dfrac{T_p + \Delta}{T_p} & \text{if } -T_p \le \Delta \le 0, \\ \dfrac{T_p - \Delta}{T_p} & \text{if } 0 \le \Delta \le T_p. \end{cases} \tag{36}$$

Since the time difference Δ can be modeled as a random variable uniformly distributed over $[-T_f, T_f]$, we have the probabilities $P(-T_p \le \Delta \le 0) = P(0 \le \Delta \le T_p) = T_p/(2T_f) = 1/(2\beta)$. The mean and variance of $\gamma(\Delta)$ are calculated in [17] and given by $E[\gamma(\Delta)] = 1/(2\beta)$ and $\mathrm{Var}[\gamma(\Delta)] \approx 1/(3\beta)$, for $\beta > 100$. The mean of W_I is m_I which can be calculated as

$$m_I = E\left[\sum_{l_d=1}^{L_d}\sum_{j=1}^{N_s}\sum_{k=2}^{N_u}\sqrt{E_p^{(k)}}\gamma(\Delta)\right] = L_d N_s (N_u - 1)\frac{\sqrt{E_p^{(k)}}}{(2\beta)}. \tag{37}$$

The variance of W_I is σ_I^2 which can be calculated as

$$\sigma_I^2 = \sum_{l_d=1}^{L_d}\sum_{j=1}^{N_s}\sum_{k=2}^{N_u}\left(\sqrt{E_p^{(k)}}\right)^2 \mathrm{Var}[\gamma(\Delta)] \approx \frac{L_d N_s (N_u - 1)E_p^{(k)}}{(3\beta)}. \tag{38}$$

Taking into account the AWGN component which has zero mean and variance $L_d N_s N_0/2$, the outputs of the correlators for the receiver of user n can be modeled as independent Gaussian random variables with distribution

$$\begin{aligned} \hat{\mathbf{r}}_j &\sim \mathbf{N}\left(L_d N_s \sqrt{E_p^{(1)}} + m_I, \sigma_I^2 + \frac{L_d N_s N_0}{2}\right), \quad j = n, \\ \hat{\mathbf{r}}_j &\sim \mathbf{N}\left(m_I, \sigma_I^2 + \frac{L_d N_s N_0}{2}\right), \quad j \ne n. \end{aligned} \tag{39}$$

The SNR per symbol at the output of the correlation receiver is

$$\rho_I = \frac{\left(L_d\sqrt{N_s E_s}\right)^2}{\sigma_I^2 + L_d N_s N_0/2} = \frac{3\beta L_d N_s}{(N_u - 1) + 3\beta N_s/\rho_0}, \tag{40}$$

where $N_s E_p = E_s$ and $\rho_0 = 2E_s/N_0$. When $N_u = 1$, that is, the single-user case, the outputs of the correlators after normalizing over $\sqrt{N_s}$ can be simplified as

$$\begin{aligned} \hat{\mathbf{r}}_j &\sim \mathbf{N}\left(L_d\sqrt{N_s E_p}, \frac{L_d N_0}{2}\right), \quad j = n, \\ \hat{\mathbf{r}}_j &\sim \mathbf{N}\left(0, \frac{L_d N_0}{2}\right), \quad j \ne n. \end{aligned} \tag{41}$$

This agrees well with the single-user analysis.

4.1.2. Multiple Access Error Probability. The distribution of the independent Gaussian random variables which represent the outputs of the correlators is given in (39). The multiple access error probability over AWGN channels can then be obtained from (14) by substituting $\sigma_I^2 + L_d N_s N_0/2$ for $\sigma^2 = L_d N_0/2$, giving

$$P_M = 1 - P_c, \tag{42}$$

where

$$P_c = \int_{-\infty}^{\infty} \left(\frac{1}{\sqrt{2\pi}} \int_{-\infty}^{(r_N/\sqrt{\sigma_I^2+(L_d N_s N_0/2)})} e^{-x^2/2} dx \right)^{N-1} \times p(r_N) dr_N,$$

$$p(r_N) = \frac{1}{\sqrt{2\pi(\sigma_I^2 + L_d N_s N_0/2)}} \times \exp\left(-\frac{\left(r_N - L_d N_s \sqrt{E_p^{(1)}} - m_I \right)^2}{2(\sigma_I^2 + L_d N_s N_0/2)} \right). \tag{43}$$

4.2. Multiple Access Error Probability over Indoor Fading Channels. The received signal over indoor fading channels can be modeled as

$$r(t) = \sum_{l_d=1}^{L_d} \sum_{k=1}^{N_u} \left[f_{l_d k}(t) \left(s_{l_d}^{(k)}(t - \tau_{l_d k}) \right)' + w_{l_d}(t) \right]. \tag{44}$$

The basis functions of the N cross-correlators of the correlation receiver for user 1 are

$$\varphi_{a l_d}^{(1)} = f_{l_d 1}^*(t) q\left(t - a^{(1)} T - \tau_{l_d 1} \right) \quad a = 1, \ldots, M. \tag{45}$$

Then (29) can be changed into

$$\mathbf{r}_i = \begin{cases} \sum_{l_d=1}^{L_d} |f_{l_d 1}|^2 N_s \sqrt{E_p^{(1)}} + W_{I,\text{naka}} + W, & \text{signal}, \\ W_{I,\text{naka}} + W, & \text{no signal}. \end{cases} \tag{46}$$

The MAI component $W_{I,\text{naka}}$ can be expressed as

$$W_{I,\text{naka}} = \sum_{l_d=1}^{L_d} \sum_{j=1}^{N_s} \sum_{k=2}^{N_u} v_{l_d 1} f_{l_d 1} v_{l_d k} f_{l_d k} \sqrt{E_p^{(k)}} \gamma(\Delta). \tag{47}$$

The mean of $W_{I,\text{naka}}$ is

$$m_{I,\text{naka}} = E(W_{I,\text{naka}}) = \sum_{l_d=1}^{L_d} \sum_{j=1}^{N_s} \sum_{k=2}^{N_u} E(v_{l_d 1}) E(f_{l_d 1}) E(v_{l_d k}) \times E(f_{l_d k}) \sqrt{E_p^{(k)}} E(\gamma(\Delta)) = 0, \tag{48}$$

and the variance of $W_{I,\text{naka}}$ is

$$\sigma_{I,\text{naka}}^2 = \text{Var}(W_{I,\text{naka}}) \approx \frac{\sum_{l_d=1}^{L_d} \sum_{k=2}^{N_u} N_s f_{l_d 1}^2 f_{l_d k}^2 E_p^{(k)}}{(3\beta)}. \tag{49}$$

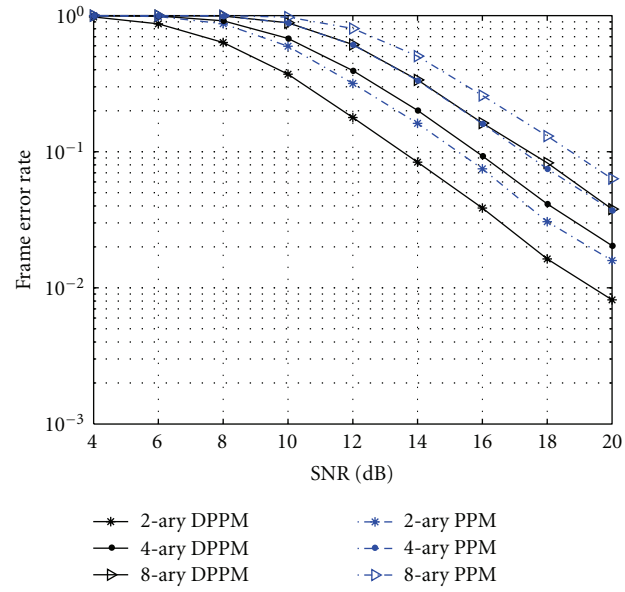

FIGURE 7: Multiple access frame error rate for an M-ary DPPM UWB system with receive diversity $L_d = 4$, and a frame length of 128 bits over a Nakagami-m fading channel, $m = 0.85$, $\beta = 500$, and $N_u = 10$.

Taking into account the AWGN component which has zero mean and variance $\sum_{l_d=1}^{L_d} f_{l_d 1}^2 N_s N_0/2$, the output of the cross-correlators of the user 1 receiver can be modeled as independent Gaussian random variables with distributions

$$\hat{\mathbf{r}}_j \sim \mathbf{N}\left(\sum_{l_d=1}^{L_d} |f_{l_d 1}|^2 N_s \sqrt{E_p^{(1)}}, \sigma_{\text{total}}^2 \right), \quad j = n,$$
$$\hat{\mathbf{r}}_j \sim \mathbf{N}(0, \sigma_{\text{total}}^2), \quad j \neq n, \tag{50}$$

where $\sigma_{\text{total}}^2 = \sum_{l_d=1}^{L_d} \sum_{k=2}^{N_u} N_s f_{l_d 1}^2 f_{l_d k}^2 E_p^{(k)}/(3\beta) + \sum_{l_d=1}^{L_d} f_{l_d 1}^2 N_s N_0/2$. The equivalent SNR is

$$\rho_{I,\text{naka}} = \frac{\left(\sum_{l_d=1}^{L_d} |f_{l_d 1}|^2 N_s \sqrt{E_p^{(1)}} \right)^2}{\sum_{l_d=1}^{L_d} \sum_{k=2}^{N_u} N_s f_{l_d 1}^2 f_{l_d k}^2 E_p^{(k)}/(3\beta) + \sum_{l_d=1}^{L_d} f_{l_d 1}^2 N_s N_0/2} = \frac{\left(\sum_{l_d=1}^{L_d} f_{l_d 1}^2 \right)^2 N_s 3\beta}{\sum_{l_d=1}^{L_d} \sum_{k=2}^{N_u} f_{l_d 1}^2 f_{l_d k}^2 + \left(\sum_{l_d=1}^{L_d} f_{l_d 1}^2 N_s 3\beta/\rho_0 \right)}. \tag{51}$$

The instantaneous SER for a multiple access UWB system with DPPM can be obtained by substituting $\rho_{I,\text{naka}}$ given by (51) in (25), and the frame error probability of a multiple access DPPM system can be obtained from (19).

5. Numerical Results

In this section, some analytical and Monte Carlo simulation results are presented to illustrate and verify the error probability expressions obtained previously.

Figure 1 compares the FER of PPM and DPPM over an AWGN channel with a frame length of 128 bits. The results for binary PPM verify the analysis given previously. This figure shows that DPPM is superior to PPM in terms of FER performance. Figure 2 shows the corresponding FER with a frame length of 512 bits. Compared with Figure 1, the FER performance is worse due to the greater number of bits in a frame, but DPPM provides a similar improvement over PPM in both cases. Figure 3 gives the FER of binary PPM and binary DPPM with receive diversity orders $L_d = 1$ and $L_d = 2$ over AWGN channels, with a frame length of 128 bits. This shows that the FER performance is improved due to the increased diversity order. For binary DPPM, there is almost a 3 dB gain with two receive antennas over one receive antenna at an FER of 10^{-2}.

Figure 4 shows the FER for 4-ary DPPM over Nakagami fading channels with different m. A larger m corresponds to improved channel conditions. As expected, the FER declines with increasing m. At an FER of 10^{-2}, there is about a 2 dB gain with $m = 1$ over $m = 0.85$, and more than a 6 dB gain with $m = 1$ over $m = 0.65$. Figure 5 shows that DPPM also has a superior FER in Nakagami fading channels. It also shows that receive diversity has a significant impact on the FER. At an FER of 10^{-1}, there is about an 8 dB gain with 4 receive antennas over 2 receive antennas for 4-ary DPPM.

Figure 6 shows the relationship between FER and the number of users for M-ary DPPM with receive diversity over AWGN channels. The FER performance of M-ary DPPM deteriorates rapidly with the number of the users due to MAI. For 8-ary DPPM, the FER is close to 10^{-1} with about 260 users. Thus M-ary DPPM is not suitable for large wireless networks with many users.

Figure 7 gives the multiple access FER of M-ary DPPM and M-ary PPM over Nakagami fading channels with receive diversity. DPPM is again superior to PPM in terms of FER performance in a multiuser environment. The FER performance of 8-ary DPPM is about the same as that of 4-ary PPM.

6. Conclusions

The error probability of DPPM over AWGN and Nakagami fading channels with receive diversity has been studied. Both single and multiuser cases were considered. The FER performance was first derived for AWGN channels and then extended to Nakagami fading channels by averaging the SNR over the channel random variable. Exact error probability expressions were derived, and Monte-Carlo simulation was employed for efficient evaluation. It was shown that for a UWB system, DPPM is superior to PPM in FER performance over both AWGN and Nakagami fading channels, and the FER performance can be significantly improved by employing receive diversity.

Acknowledgments

This work was supported by National 863 Hi-Tech Research and Development Program of China under Grant no. 2007AA12Z317, New Century Educational Talents Plan of Chinese Education Ministry under Grant no. NCET-08-0504, and Shandong province Nature Science Foundation under Grant no. JQ200821.

References

[1] A. J. C. Moreira, R. T. Valadas, and A. M. de Oliveira Duarte, "Performance evaluation of the IEEE 802.11 infrared physical layer," in *Proceedings of the International Symposium on Communication Systems and Digital Signal Processing*, pp. 10–15, 1998.

[2] J. M. H. Elmirghani and R. A. Cryan, "Analytic and numeric modelling of optical fibre PPM slot and frame spectral properties with application to timing extraction," *IEE Proceedings: Communications*, vol. 141, no. 6, pp. 379–389, 1994.

[3] B. Wilson, Z. F. Ghassemlooy, and E. D. Kaluarachchi, "Digital pulse interval modulation for fiber transmission," in *Collision Avoidance and Automated Traffic Management Sensors*, Proceedings of SPIE, pp. 53–59, October 1995.

[4] E. D. Kaluarachchi, Z. Ghassemlooy, and B. Wilson, "Digital pulse interval modulation for transmission over optical fibre with direct detection," in *All-Optical Communication Systems: Architecture, Control and Network Issues II*, Proceedings of SPIE, pp. 98–105, November 1996.

[5] E. D. Kaluarachchi, *Digital pulse interval modulation for optical communication systems*, Ph.D. thesis, Sheffield Hallam University, Sheffield, UK, 1997.

[6] Z. Ghassemlooy, A. R. Hayes, N. L. Seed, and E. D. Kaluarachchi, "Digital pulse interval modulation for optical communications," *IEEE Communications Magazine*, vol. 36, no. 12, pp. 95–99, 1998.

[7] D. S. Shiu and J. M. Kahn, "Differential pulse-position modulation for power-efficient optical communication," *IEEE Transactions on Communications*, vol. 47, no. 8, pp. 1201–1210, 1999.

[8] U. Sethakaset and T. A. Gulliver, "Differential amplitude pulse-position modulation for indoor wireless optical communications," *EURASIP Journal on Wireless Communications and Networking*, vol. 2005, Article ID 542578, 9 pages, 2005.

[9] L. Zhao and A. M. Haimovich, "Capacity of M-ary PPM ultra-wideband communications over AWGN channels," in *Proceedings of the IEEE Vehicular Technology Conference (VTC '01)*, pp. 1191–1195, October 2001.

[10] F. Ramirez-Mireles and R. A. Scholtz, "Multiple-access performance limits with time hopping and pulse position modulation," in *Proceedings of the IEEE Military Communications Conference*, pp. 529–533, October 1998.

[11] H. Zhang, T. Udagawa, T. Arita, and M. Nakagawa, "A statistical model for the small-scale multipath fading characteristics of ultrawide band in-door channel," in *Proceedings of the IEEE Conference on Ultra Wideband Systems and Technologies*, pp. 81–85, May 2002.

[12] J. G. Proakis, *Digital Communications*, McGraw-Hill, New York, NY, USA, 4th edition, 2001.

[13] A. R. Hayes, Z. Ghassemlooy, and N. L. Seed, "Optical wireless communication using digital pulse interval modulation," in *Proceedings of the Optical Wireless Communications*, vol. 3532 of *Proceedings of SPIE*, pp. 61–69, Boston, Mass, USA, November 1998.

[14] H. Zhang and T. A. Gulliver, "Performance and capacity of PAM and PPM UWB time-hopping multiple access communications with receive diversity," *EURASIP Journal on Applied Signal Processing*, vol. 2005, no. 3, pp. 306–315, 2005.

[15] M. Z. Win and R. A. Scholtz, "Ultra-wide bandwidth time-hopping spread-spectrum impulse radio for wireless multiple-access communications," *IEEE Transactions on Communications*, vol. 48, no. 4, pp. 679–691, 2000.

[16] G. Durisi and G. Romano, "On the validity of Gaussian approximation to characterize the multiuser capacity of UWB TH PPM," in *Proceedings of the IEEE Conference on Ultra Wideband systems and Technologies (UWBST '02)*, pp. 157–161, May 2002.

[17] L. Zhao and A. M. Haimovich, "The capacity of an UWB multiple-access communications system," in *Proceedings of the IEEE International Conference on Communications (ICC '02)*, pp. 1964–1968, May 2002.